THE JOURNAL OF BIOLOGICAL CHEMISTRY VOL. 290, NO. 14, pp. 8938–8948, April 3, 2015

MicroRNA-873 (MiRNA-873) Inhibits Glioblastoma Tumorigenesis and Metastasis by Suppressing the Expression of IGF2BP1

Received for publication, November 11, 2014, and in revised form, February 2, 2015 Published, JBC Papers in Press, February 10, 2015, DOI 10.1074/jbc.M114.624700

Ren-jie Wang[‡1], Jian-wei Li[§1], Bu-he Bao[‡], Huan-cheng Wu[§], Zhen-hua Du[‡], Jing-liang Su[§], Ming-hua Zhang[‡], and Hai-qian Liang[§2]

From the Departments of [‡]Clinical Laboratory and [§]Neurosurgery, Pingjin Hospital, Logistics College of Armed Police Forces, Tianjin 300162, China

Background: Recent research has uncovered tumor-suppressive and oncogenic potential of miRNAs.
Results: miR-873 suppresses the proliferation, migration, and invasiveness of GBM cells by targeting IGF2BP1.
Conclusion: Down-regulation of miR-873 results in overexpressed IGF2BP1, contributing to tumorigenesis of GBM cells.
Significance: The identification of tumor suppressor miR-873 and its oncogenic target IGF2BP1 in GBM cells is potentially valuable for cancer diagnosis and therapy.

Glioblastoma multiforme (GBM) is known as a highly malignant brain tumor with a poor prognosis, despite intensive research and clinical efforts. In this study, we observed that microRNA-873 (miR-873) was expressed at low levels in GBM and that the overexpression of miR-873 dramatically reduced the cell proliferation, migration, and invasion of GBM cells. Our further investigations of the inhibition mechanism indicated that miR-873 negatively affected the carcinogenesis and metastasis of GBM by down-regulating the expression of IGF2BP1, which stabilizes the mRNA transcripts of its target genes. These results demonstrate that miR-873 may constitute a potential target for GBM therapy.

Gliomas are typed into four grades (I, II, III, IV) based on the different histological features of tumors (1). Glioblastoma multiforme (GBM)[3] tumors, known as Grade IV gliomas, are the most aggressive and malignant primary tumors (2). GBM is characterized by aggressive vascular proliferation, invasiveness, inherent resistance to standard therapies, stem cell-like behavior, and normal brain necrosis (3, 4). The median life expectancy of newly diagnosed patients is less than 1 year, and the 5-year survival rate is less than 3% (5). Although increasing evidence has revealed different aspects of the molecular mechanism of GBM, the detailed molecular signaling pathways in GBM remain to be explored.

MicroRNAs (miRNAs) are a class of non-coding RNA molecules consisting of 20–22 nucleotides that regulate the expression of special genes in a posttranscriptional manner (6, 7). Various microRNAs have been found to participate in the progression of gliomas (8, 9). For instance, miR-21 acts as an anti-apoptotic factor in GBM by targeting the p53 network (8–10); miR-10b is involved in the cell cycle and programmed cell death via regulating the expression of Bim, TFAP2C, p16, and p21 (11); miR-218 inhibits cell migration, invasion, proliferation, and stem-like qualities by targeting Bmi1 (12); miR-195 negatively regulates the proliferation of glioma cells by down-regulating the expression of cyclin D1 and cyclin E1 (13); miR-137 inhibits the growth of glioma cells by directly targeting Rac1 (14); and miR-16 functions as a tumor suppressor gene in glioma growth and invasiveness via the inhibition of BCL2 and the NF-KB1/MMP-9 signaling pathway (15). All of these miRNAs play important roles in the development of the malignant GBM phenotype. However, few studies have examined miR-873, a novel miRNA, in GBM development. In this study, we discovered that the low level of miR-873 in GBM was associated with the carcinogenesis and metastasis of GBM via the promotion of IGF2BP1 protein expression.

EXPERIMENTAL PROCEDURES

Glioma Tissues and Cell Lines—Human GBM and their adjacent normal tissues were obtained from six patients. The tissues used for RNA extraction were flash-frozen in liquid nitrogen and stored at −80 °C. Written informed consent was acquired from each patient, and this research was approved by the Pingjin Hospital Medical Ethics and Human Clinical Trial Committee. Glioma cell lines (A172, T98G, U87, U373, U251, and U138) were purchased from the American Type Culture Collection and grown in DMEM medium supplemented with 10% FBS. The cells were maintained in a humidified atmosphere at 37 °C with 5% CO_2.

3-(4, 5-Dimethylthiazol-2-yl)-2,5-diphenyltetrazolium Bromide (MTT) Assays—MTT assays were carried out to assess cell viability. Briefly, U87 and U373 cells were seeded at a concentration of 10^4 cells/well in a 96-well plate. miRNA mimic, negative control RNA, or eukaryotic expression plasmids were transfected into the cells using Lipofectamine 2000 the following day

[1] Both authors contributed equally to this work.
[2] To whom correspondence should be addressed: Dept. of Neurosurgery, Pingjin Hospital, Logistics College of Armed Police Forces, Number 220, Chenglin Rd., Tianjin 300162, China. Tel.: 86-02260577125; Fax: 86-02260577125; E-mail: lianghaiqian711@163.com.
[3] The abbreviations used are: GBM, glioblastoma multiforme; miRNA, microRNA; miR-873, microRNA-873; IGF2BP1, insulin-like growth factor 2 mRNA-binding protein 1; MTT, 3-(4, 5-dimethylthiazol-2-yl)-2,5-diphenyltetrazolium bromide; mfe, minimum free energy; PTEN, phosphatase and tensin homolog; mut, mutant.

according to the manufacturer's protocol. The cells were cultured at 37 °C in transfection medium for 6 h. The medium was then replaced with complete medium containing MTT (final concentration, 250 μg/ml) for the subsequent assays. The plates were incubated for an additional 12, 24, or 48. The trapped MTT crystals in the cells were solubilized in 200 μl of dimethyl sulfoxide (DMSO) at 37 °C for 15 min. The absorbance was determined in a microtiter plate reader (Molecular Devices, Menlo Park, CA) at 570 nm, with 650 nm as the reference wavelength. All experiments were performed in triplicate.

Wound-healing and Invasion Assays—The wound-healing assays were performed as follows. The cells were seeded in six-well plates and cultured to 100% confluence. A wound was then produced in the cell monolayer using a plastic pipette tip. The cells were then washed in PBS buffer and cultured for another 48 h. The wound closure rate was then observed and described using a percentage. Cells suspended in serum-free medium (10^5) were placed into the upper chamber of an insert precoated with Matrigel (BD Biosciences), and DMEM supplemented with 10% fetal bovine serum was added to the lower chamber. The cells were allowed to invade for 48 h. The cells remaining on the upper surface of the membrane were removed, whereas the cells that had invaded through the membrane were stained with 20% methanol and 0.2% crystal violet, imaged, and counted under a microscope (Olympus, Tokyo, Japan).

Colony Formation Assays—For the colony formation assays, the cells were harvested and seeded at a density of 200 cells/well in 12-well plates and incubated at 37 °C and 5% CO_2 in a humidified incubator for 2 weeks. During colony growth, the culture medium was replaced every 3 days. The colony number in each well was counted and calculated.

Flow Cytometry Analysis—Glioma cells were harvested using trypsinization, washed in ice-cold PBS, and then fixed in 80% ice-cold ethanol in PBS. Before staining, the cells were pelleted in a chilled centrifuge and resuspended in cold PBS to a concentration of 1×10^4 cells. Bovine pancreatic RNase (Sigma-Aldrich) was added to a final concentration of 2 mg/ml, and the cells were incubated at 37 °C for 30 min. To detect the cell cycle distribution, the cells were stained with 20 mg/ml propidium iodide (Sigma-Aldrich) for 20 min at room temperature. For the cell apoptosis assays, the cells were labeled using the annexin V-FITC apoptosis detection kit (Invitrogen) as described by the manufacturer. The cell cycle profiles and the cell apoptosis rates were quantified using a flow cytometer (Beckman-Coulter).

Transwell Assays—For the Transwell migration assays, 10^5 cells were suspended in medium without serum and placed on the top side of a polycarbonate Transwell filter without Matrigel in the upper chamber of a QCM^{TM} 24-well cell invasion assay plate (Cell Biolabs, Inc.); medium without serum was used in the lower chamber. For the invasion assays, the experimental procedures were similar to that for the migration assays, except that the filters were coated with Matrigel. The cells were incubated at 37 °C for 8 h for the migration assays or 48 h for the invasion assays. The cells in the top chambers were removed with cotton swabs. The migrated and invaded cells on the lower membrane surface were washed twice with PBS buffer and fixed in in 4% paraformaldehyde for 30 min. The well was stained with 0.1% crystal violet for 20 min after another wash using PBS buffer. Following at least three washes in double-distilled H_2O, the membrane was dried and observed under a light microscope. The assays were performed in triplicate, and the data are presented as the means ± S.E.

Xenografted Tumor Model—Five pairs of the BALB/c nude mice were used. In general, 3×10^6 U87 cells (without transfection miRNA mimics or control mimics) were suspended in 150 μl of serum-free DMEM for each mouse. The right dorsal flank of each nude mouse was then subcutaneously injected with 3×10^6 U87 cells to establish a xenograft. The tumors formed 1 week later. Ten tumor-bearing nude mice were randomly divided into two groups (miR-873 and control). The tumor was then injected with a mixture of miR-873 mimics and Lipo-2000 (transfection reagent) or a mixture of control mimics and Lipo-2000. We repeated this injection every 4 days. The animals were sacrificed after 28 days. The nude mice were handled and cared for according to the National Institutes of Health Animal Care and the Use Committee guidelines of the Experiment Animal Center of Pingjin Hospital, Tianjin, China).

Bioinformatics Methods—The miRNA targets predicted by computer-aided algorithms were obtained from miRanda – mirSVR, miRDB, miRWalk, and targetscan. The minimum free energy (mfe) structures of the RNA duplexes formed by miR-873, and its putative binding sequences were obtained using RNAhybrid.

Western Blot—The total protein was extracted from cells using radioimmunoprecipitation assay lysis buffer supplemented with protease inhibitor cocktail (Roche Applied Science) and PMSF (Roche Applied Science). The protein concentration was measured using a BCA protein assay (Pierce) and a NanoDrop 2000c spectrophotometer (Thermo Scientific). The total protein extracts were separated via 12% SDS-PAGE and then transferred to nitrocellulose membranes. The IGF2BP1 protein was probed with specific antibodies obtained from Proteintech Co. Ltd. after the blot was blocked with 5% nonfat milk. The gray intensities of the protein bands were quantified using the ImageJ software. GAPDH antibody was purchased from Sigma.

Immunohistochemistry Assays—The sections of GBM cancer tissues and matched normal controls were mechanically deparaffinized and incubated in target retrieval solution (Dako, Carpentaria, CA) at 95 °C for 40 min. After the endogenous peroxidase activity was blocked with methanol containing 3% hydrogen peroxide (Dako) for 30 min, the tissue sections were incubated with primary antibody to IGF2BP1 at 4 °C overnight. The sections were then incubated in secondary antibody at 37 °C for 60 min. Subsequently, the sections were counterstained with hematoxylin for 1 min.

Statistical Analysis—The data are presented as the mean ± S.D. A Student's t test was used to evaluate significant differences, and $p < 0.05$ was considered statistically significant.

RESULTS

The Expression of miR-873 Was Down-regulated in GBM—A previous study revealed via high-throughput sequencing that miR-873 was down-regulated in GBM (16). To further assess the miR-873 expression in GBM and normal adjacent tissue, we

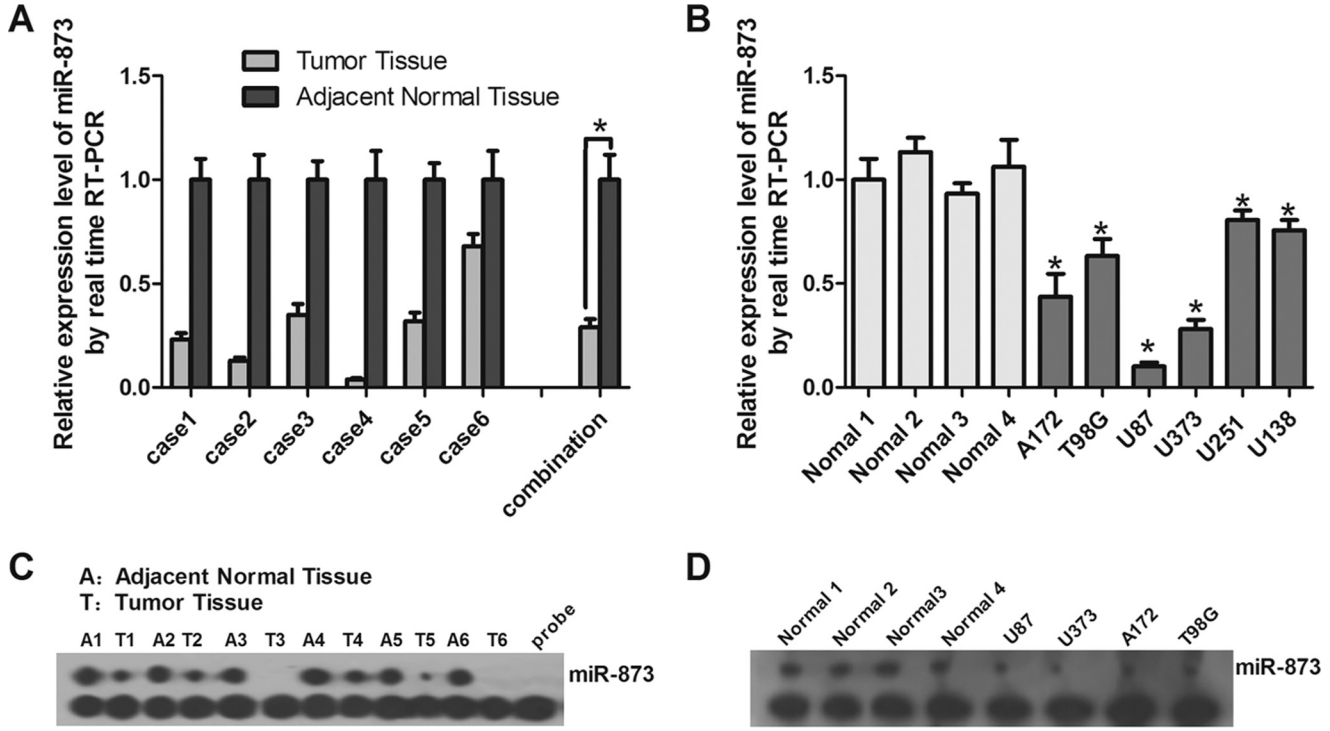

FIGURE 1. **Analysis of miR-873 in GBM tissues and adjacent normal tissues.** *A*, the relative expression level of mature miR-873 in six pairs of tumor issues and adjacent normal counterparts using real-time RT-PCR. The lines represent the means of independent experiments in each group. * indicates $p < 0.005$. *B*, the relative levels of miR-873 were measured in four normal human astrocytes and six GBM cell lines, A172, T98G, U87, U373, U251, and U138. *Error bars* represent S.E. * indicates $p < 0.05$ *versus* normal. *C* and *D*, miR-873 expression detected by primer extension. T98G, A172, U373, and U87 are glioblastoma cell lines. 5 mg of total RNA were used for each reaction. Free probe is shown as a negative control. Primer extension reactions were resolved on 15% Tris-borate-EDTA-urea polyacrylamide gels and exposed to film for 50 min.

measured its expression levels in six GBM tumor tissues and their adjacent counterparts in pairs using real-time RT-PCR and primer extension assay. As shown in Fig. 1*A*, the miR-873 expression in malignant tumor tissue was markedly lower than that in non-cancerous tissue. Specifically, the average expression level of miR-873 in GBM was only 0.25-fold that of the adjacent normal tissues. To further confirm this result, we detected the expression level of miR-873 in four normal brain tissues and six GBM cell lines, A172, T98G, U87, U373, U251, and U138, using real-time RT-PCR and primer extension assay and observed that normal brain tissues expressed significantly more miR-873 than GBM cell lines (Fig. 1*B*). These data indicated that miR-873 was down-regulated in GBM and may act as a tumor suppressor.

Up-regulation of miR-873 Inhibits GBM Cell Proliferation but Induces Apoptosis—To confirm that miR-873 plays a tumor suppressor role in GBM, two GBM cell lines, U373 and U87, were transfected with miR-873 mimics that shared sequences with mature miR-873. The levels of miR-873 can be significantly elevated in the U373 and U87 cells after transfection (Fig. 2*A*). The effect of the increased level of miR-873 on U373 and U87 cell proliferation was determined using MTT and colony formation assays. The results of the MTT assay demonstrated that miR-873 could inhibit the viability of GBM cells, whereas the results of the colony formation assays suggested that miR-873 overexpression could also reduce anchorage-independent growth in GBM cells (Fig. 2, *B–E*). The analysis of the cell cycle kinetics using flow cytometry indicated that miR-873 significantly induced cell cycle arrests in both U87 and U373 cells. The G_0/G_1 phase fractions of U87 cells and U373 cells transfected with miR-873 increased by 25 and 17%, respectively, when compared with the phase fractions of corresponding cells transfected with miR-control mimics. Moreover, the decrease in S phase populations of both cell lines transfected with miR-873 mimics exceeded 50% when compared with the control group (Fig. 2, *F* and *G*). The marked G_0/G_1 arrest and decrease in the S phase fraction suggested that miR-873 may act as an inhibitor by inducing cell apoptosis. To further confirm this assumption, we measured and compared the apoptosis ratios of U87 and U373 cells transfected with miR-873 mimics with the ratios of the corresponding cells with miR-control mimics using flow cytometry. We discovered that the number of apoptotic cells labeled with annexin V or 7-aminoactinomycin D increased by 1- and 0.53-fold in U87 and U373 cells, respectively, after miR-873 mimic treatment (Fig. 2*H*). To investigate the function of miR-873 in glioma carcinogenesis, we further assessed the influence of the elevated level of miR-873 in cells on the tumor-forming potential *in vivo*. Three million U87 cells transfected with either miR-873 or miR-control mimics were implanted into the right flanks of nude mice by subcutaneous injection. The mean volumes of xenograft tumors were measured every week. Four weeks after the injection, the xenograft tumors were excised and measured *in vitro*. We found that cells transfected with miR-873 generated smaller tumors than cells transfected with miR-control mimics ($n = 5$ animals/group, $p < 0.05$) (Fig. 2, *I* and *J*). Thus, we suggest that the transfection of miR-873 into GBM cells inhibits tumor cell proliferation *in vitro* and *in vivo*.

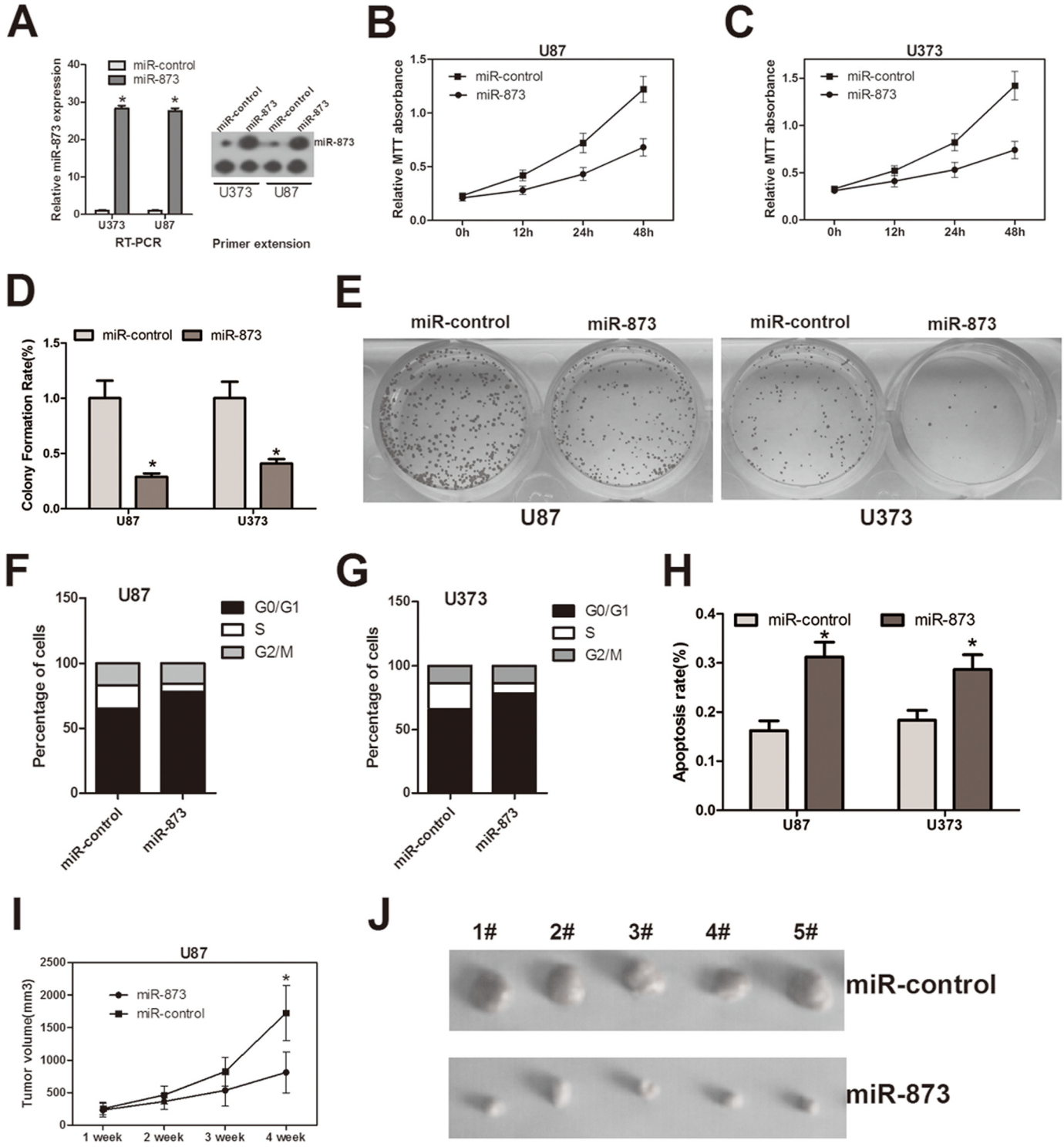

FIGURE 2. **The increased level of miR-873 inhibits the proliferation but induces the apoptosis of glioma cells *in vitro*.** *A*, the relative levels of miR-873 in two GBM cell lines, U87 and U373, were determined after the cells were transfected with miR-873 mimics or miR-control mimics using real-time RT-PCR and primer extension assay. *B*, the relative cell viability in U87 cells was measured after the cells were transfected with miR-873 mimics or miR-control mimics using MTT assays. *C*, the relative cell viability of U373 cells was detected using MTT assays after the cells were transfected with miR-873 mimics or miR-control mimics. *D*, the colony formation of miR-873-U87 cells and miR-873-U373 cells was quantified and compared with that of the GBM cells transfected with miR-control mimics in their respective groups. *E*, the representative micrographs of the colony formation assays are shown. *F*, the cell cycle distributions of the U87 cells transfected with miR-873 mimics or miR-control mimics were detected and compared. *G*, the cell cycle distributions of the U373 cells transfected with miR-873 mimics or miR-control mimics were detected and compared with each other. *H*, the apoptosis rate of the two GBM cell lines transfected with miR-873 mimics were measured and compared with that of the cells transfected with miR-control mimics. Each bar or point represents the mean of three independent experiments. *I*, the U87 GBM tumor growth *in vivo* was determined based on the tumor volume, which was calculated based on weekly measurements after injection. *J*, a representative image of *in vivo* tumor growth is shown. In this panel, the weights of the tumors generated from the GBM cells transfected with miR-873 mimic in three nude mice were measured and compared with the control groups. *Error bars* represent S.E. * means $p < 0.05$.

Up-regulation of miR-873 Inhibits GBM Cell Migration and Invasion—Transwell migration assays were utilized to examine the effect of miR-873 on cell migration and invasion. The migration level of the U87 and U373 cells transfected with miR-873 mimics only reached ~35% of the level of the cells transfected with miR-control mimics (Fig. 3, *A* and *B*). Similarly, the invasive potential of the U87 and U373 cells decreased by 0.8-fold after transfection with miR-873 mimics when compared with the potential after transfection with miR-control mimics (Fig. 3, *C* and *D*). Furthermore, the quantification of wound closure showed that U87 cells transfected with miR-873 mimics closed 10.1% of the wound after 24 h and 39.1% of the wound after 48 h. However, U87 cells transfected with miR-control mimics closed 59.7% of the wound after 24 h and 99.2% of the wound after 48 h (Fig. 3*E*). In the other group, U373 cells transfected with miR-373 mimics closed 25.6% of the wound after 24 h and 61.1% of the wound after 48 h. Moreover, U373 cells transfected with control mimics closed 51.1% of the wound after 24 h and 99.4% of the wound after 48 h (Fig. 3*F*). These data suggest that the increased levels of miR-873 in GBM cells significantly inhibited both cell migration and invasion.

IGF2BP1 Is Characterized as a Target of miR-873—MicroRNAs inhibit gene expression by binding to the mRNA transcript of the target gene to induce its degradation. To identify novel miR-873 target genes, four cited algorithms, miRanda – mirSVR, miRDB, miRWalk, and Targetscan, were used to predict the potential targets of miR-873. As a result, a potential list of targets including 21 genes was identified. Among these genes, IGF2BP1 is up-regulated in a large number of malignancies, which led us to believe that IGF2BP1 may be a direct target of miR-873 in GBM (Fig. 4*A*). Three putative binding sites of the microRNA in the 3′-UTR of IGF2BP1 (IGF2BP1-3′-UTR WT) are described in Fig. 4*B*, and the complementary seed sequences were mutated as described in the figure legend to generate the 3′-UTR mutant (IGF2BP1-3′-UTR mut), which should not bind miR-873. Moreover, we obtained three mfe structures of the RNA duplexes formed by miR-873 and its putative binding sequences using RNAhybrid and found that the miR-873 and the first putative binding site duplex featured a lower mfe than the two other duplexes (Fig. 4*A*). The lower mfe suggested that miR-873 might bind to the 3′-UTR of IGF2BP1 at the first putative binding site. We conducted luciferase reporter assays to confirm this hypothesis. As shown in Fig. 4*C*, the luciferase activity generated by the reporter vector with IGF2BP1-3′-UTR WT decreased by 52.4% after co-transfection with miR-873 when compared with the control group. However, the activity generated by the reporter vector with IGF2BP1-3′-UTR mut-1 was slightly higher than that of the control group after the co-transfection with miR-873. Furthermore, the mutation of the second and third binding sites in the 3′-UTR of IGF2BP1 did not affect the activity generated by the reporter vectors when compared with the control groups (Fig. 4*C*). These results indicated that miR-873 might suppress the expression of IGF2BP-1 by strongly and directly binding to the first putative site in its 3′-UTR. The following Western blot assays showed that the relative protein level of IGF2BP1 in U87 and U373 decreased by 81.3 and 73.4%, respectively, after transfection with miR-873; GAPDH was used as an internal control (Fig. 4*D*). However, the addition of an miR-873 antagonist increased the IGF2BP1 expression level (Fig. 4*D*). Similarly, the mRNA level of IGF2BP1 determined using real-time PCR in U87 and U373 decreased by 51.3 and 49.7%, respectively, after miR-873 transfection (Fig. 4*E*).

Up-regulation of IGF2BP1 Reverses the Suppressive Effect of miR-873 on the Advance of GBM Cells—To overexpress IGF2BP1 in GBM cells, we transfected the cells with pcMV6/IGF2BP1 vectors. The protein level of IGF2BP1 increased 4.51-fold in U87 cells co-transfected with miR-873 mimics and pcMV6/IGF2BP1 when compared with the protein level in the cells co-transfected with miR-873 and the control vector, pcMV6. Similarly, the overexpression of IGF2BP1 increased the protein level in U373 transfected with miR-873 mimics and pcMV6/IGF2BP1 by 6.67-fold when compared with the level in cells transfected with miR-873 mimics and pcMV6 (Fig. 5, *A* and *B*). These results suggested that overexpressing IGF2BP1 using the pcMV6/IGF2BP1 vector in GBM cells could partially rescue the down-regulation of IGF2BP1 expression caused by the increased cellular level of miR-873. The viability of GBM cells transfected with miR-873 mimics and pcMV6/IGF2BP1 was determined with an MTT assay. The absorbance increased 0.19-fold in U87 and 0.23-fold in U373 cells when IGF2BP1 expression was up-regulated when compared with the viability of the cells transfected with miR-873 and pcMV6, respectively (Fig. 5*C*). Moreover, the number of colonies formed by U87 and by U373 cells overexpressing the IGF2BP1 protein increased by 1.85- and 1.84-fold when compared with the number of colonies formed by the corresponding cells transfected with miR-873 mimics and pcMV6, respectively (Fig. 5, *D* and *E*). IGF2BP1 overexpression decreased the apoptosis rate of U87 cells expressing miR-873 by 0.27-fold and decreased the rate of U373 cells by 0.07-fold (Fig. 5*F*). The Transwell migration system showed that the percentage of migrated U87 cells co-transfected with miR-873 mimics and pcMV6/IGF2BP1 increased 1.17-fold and that of migrated U373 cells increased 0.98-fold when compared with their counterparts co-transfected with miR-873 and pcMV6 (Fig. 5*G*). In line with the previous data, the up-regulation of IGF2BP1 expression increased the invasiveness of U87 cells and U373 cells transfected with miR-873 mimics by 1.3- and 2.12-fold, respectively (Fig. 5*H*).

High Level of miR-873 Decreased the mRNA Level of MKI67, c-MYC, PTEN, and CD44—IGF2BP1 helps to stabilize the mRNA transcript. As described previously, the binding of IGF2BP1 to c-MYC and MKI67 mRNA prevented mRNA degradation and increased mRNA expression (17–19); the stabilization of CD44 mRNA was attributed to the 3′-UTR of the transcript, which was bound by IGF2BP1 protein (20); PTEN mRNA was identified as a novel target transcript of IGF2BP1 and decayed faster in cells upon IGF2BP1 knockdown (21). To verify that the down-regulation of IGF2BP1 expression due to the up-regulation of miR-873 in GBM cells could destabilize c-MYC, MKI67, CD44, and PTEN mRNA, we measured the mRNA levels of these potential target transcripts of IGF2BP1. The real-time RT-PCR assays showed that the cellular level of MKI67 mRNA and c-MYC mRNA decreased by 0.61- and 0.53-fold in U87 cells, respectively, when compared with the level in the control group, in which the tumor cells were transfected

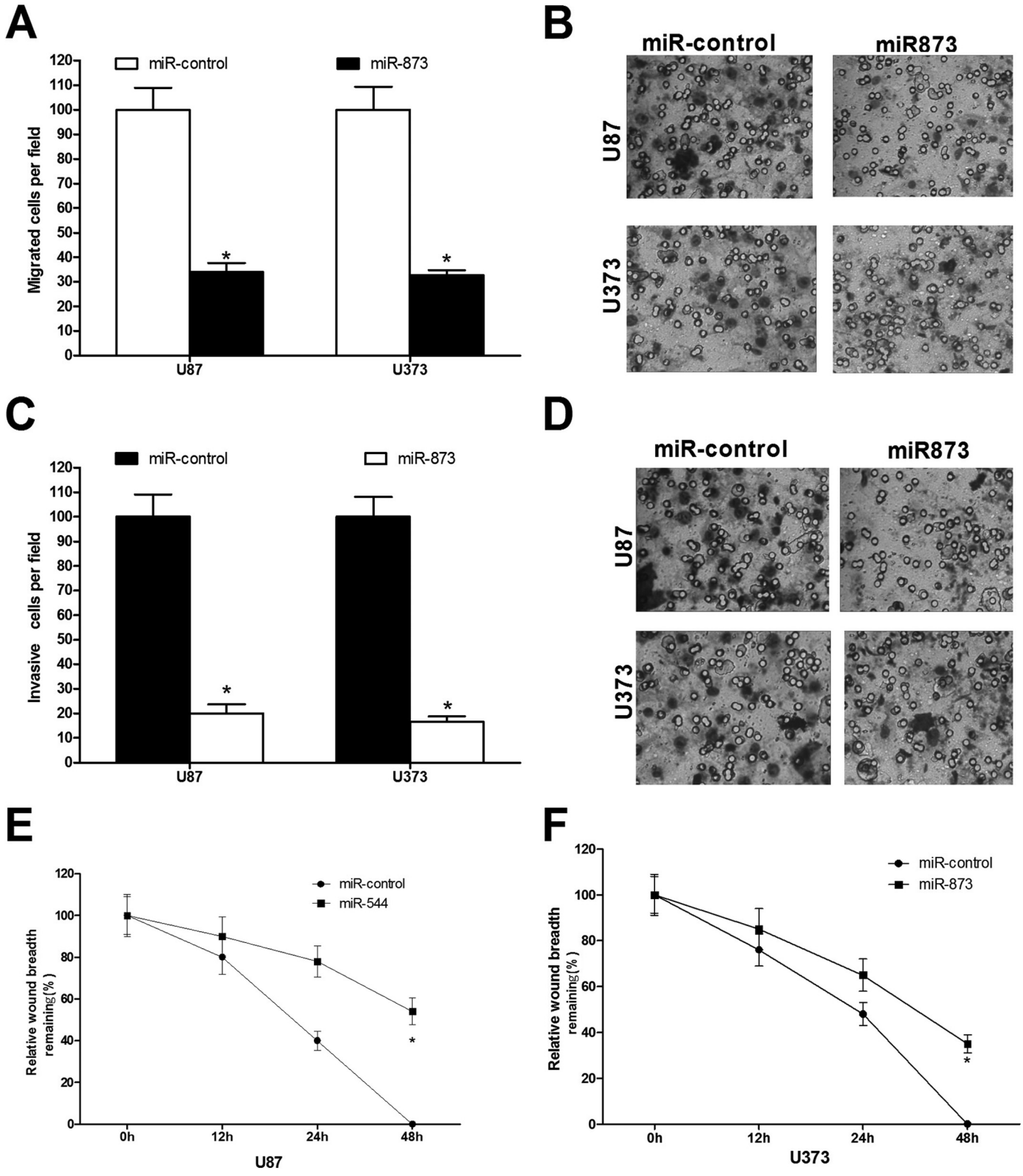

FIGURE 3. **The transfection of GBM cells with miR-544 inhibits the migration and invasion of the cells *in vitro*.** *A*, the migration abilities of miR-873-U87 cells and miR-873-U373 cells were quantified and compared with that of the cells transfected with miR-control mimics in their respective groups. *B*, the representative micrographs of the migration of miR-873-U87 cells and miR-873-U373 cells are shown. *C*, the invasiveness of miR-873-U87 cells and miR-873-U373 cells was quantified and compared with that of cells transfected with miR-control mimics in their respective groups. *D*, the representative micrographs of the invasion of miR-873-U87 and miR-873-U373 cells are shown. *E*, the wound-healing assay showed that the migration of miR-873-U87 cells differed from that of cells transfected with miR-control mimics at different time points. *F*, the wound-healing assay showed that the migration of miR-873-U373 cells differed from that of cells transfected with miR-control mimics at different time points. The motility is expressed as the percentage of migration at the zero time point. Each bar represents the mean of three independent experiments. *Error bars* represent S.E. * indicates $p < 0.05$.

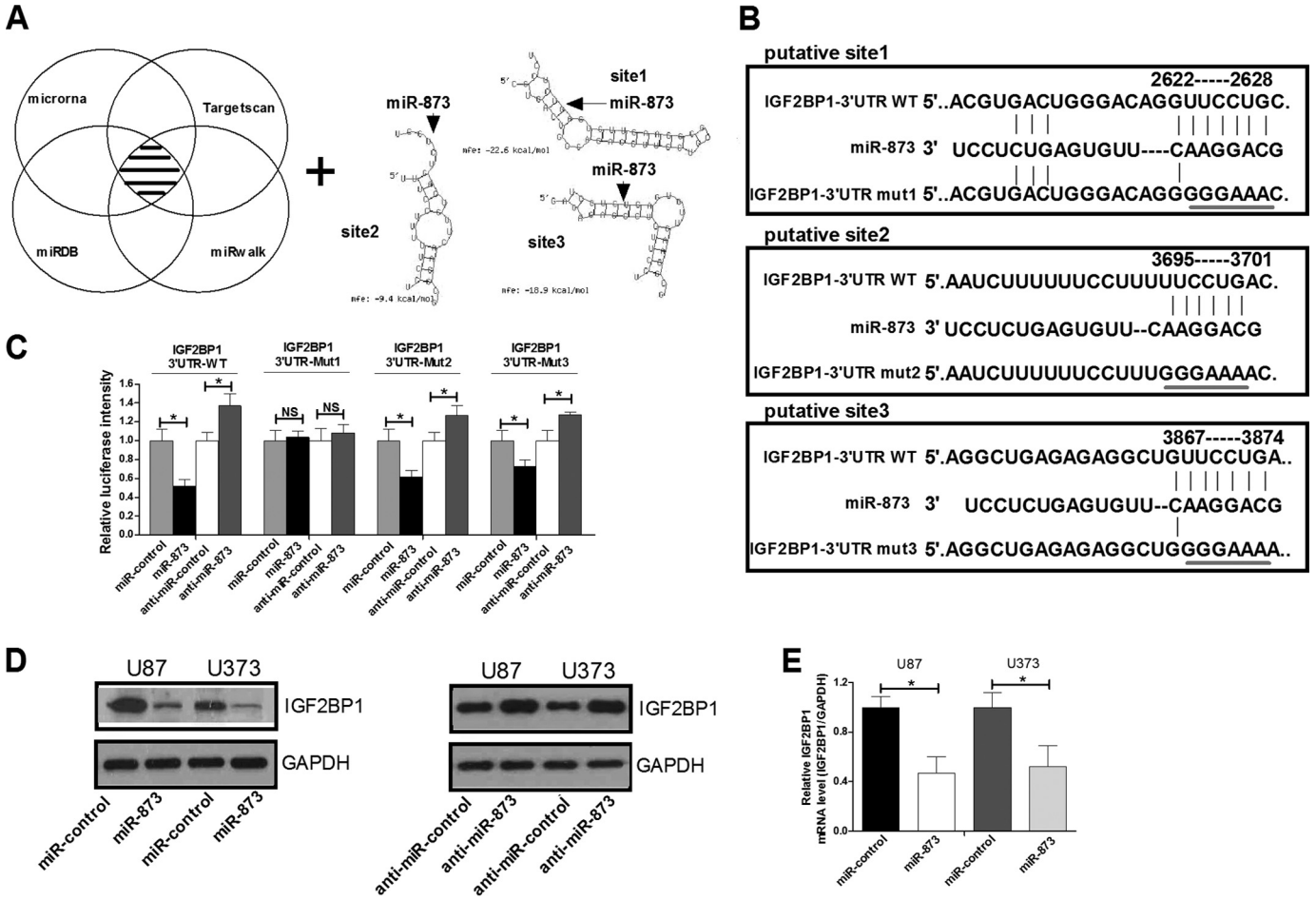

FIGURE 4. **miR-873 directly targeted the IGF2BP1 gene.** *A*, the potential targeted genes are listed based on the predictions by the four algorithms. The gene to be further analyzed, IGF2BP1, was within the *shaded area*. The structures of the RNA duplexes formed by miR-873 and its putative binding sequences with the predicted mfe were located on the *right*. *B*, the 3′-UTR fragments of IGF2BP1 gene and its mutant are indicated in *boxes*. The putative base pair region is labeled with *vertical lines* between the words representing the bases. *C*, the relative firefly activities generated by the luciferase reporter plasmids containing wild-type or mutant IGF2BP1 3′-UTR in GBM cells with miR-873 or control mimics were determined using the Dual-Luciferase assays. *D*, Western blot analyses of the IGF2BP1 protein level were performed following treatment of U87 cells and U373 cells with miR-873, anti-miR-873, or controls. *E*, quantitative RT-PCR analyses of the IGF2BP1 mRNA level were performed following the treatment of U87 cells and U373 cells with miR-873 or control mimics. GAPDH was used as a control. *Error bars* indicate S.D. *, $p < 0.05$.

with miR-control mimics rather than miR-873 mimics (Fig. 6*A*). Moreover, the amount of PTEN mRNA and CD44 mRNA decreased by 0.78- and 0.81-fold in U87 cells (Fig. 6*B*). Furthermore, transfecting U373 cell with miR-873 mimics decreased the target transcripts when compared with the level in the control group (Fig. 6, *C* and *D*). These results suggested that miR-873 might decrease the level of c-MYC, MKI67, CD44, and PTEN mRNA by down-regulating the expression of the IGF2BP1 gene in GBM cells. Furthermore, the following Western blotting assays showed that the low level of target transcripts corresponded to a low level of protein expression in GBM cells (Fig. 6, *E* and *F*).

The Down-regulation of miR-873 Expression Induced IGF2BP1-mediated Carcinogenesis and Metastasis—Because IGF2BP1 overexpression partially mitigated the negative impact of miR-873 mimics on the progression of GBM, the molecular mechanism of the inhibition of miR-873 during the carcinogenesis and metastasis of GBM may involve the dysregulation of IGF2BP1 expression. To prove this hypothesis, we determined the expression level of IGF2BP1 mRNA and protein in GBM. The IGF2BP1 expression levels were significantly higher in tumor tissues than in corresponding normal adjacent tissues (Fig. 7*A*). Furthermore, the expression of IGF2BP1 mRNA was also increased in GBM cell lines, including A172, T98G, U87, U373, U251, and U138, when compared with the expression in normal brain tissue (Fig. 7*B*). Moreover, we observed a significant negative correlation between the IGF2BP1 mRNA levels and miR-873 levels ($r = -0.9480$, $p < 0.05$) in GBM tissues (Fig. 7*C*). The inverse relationship indicated that when IGF2BP1 turnover is decreased (more IGF2BP1 mRNA), miR-873 levels are decreased. The immunohistochemistry staining of tissue sections showed that the IGF2BP1 level was markedly higher in GBM tissues than in normal tissue (Fig. 7*D*). These data support that the down-regulation of miR-873 expression in GBM induced carcinogenesis and metastasis by promoting the expression of IGF2BP1, which stabilizes the mRNA transcripts of c-MYC, MKI67, PTEN, and CD44. Furthermore, the stabilization of the target mRNAs of IGF2BP1 ultimately promoted the expression of the corresponding genes (Fig. 7*E*).

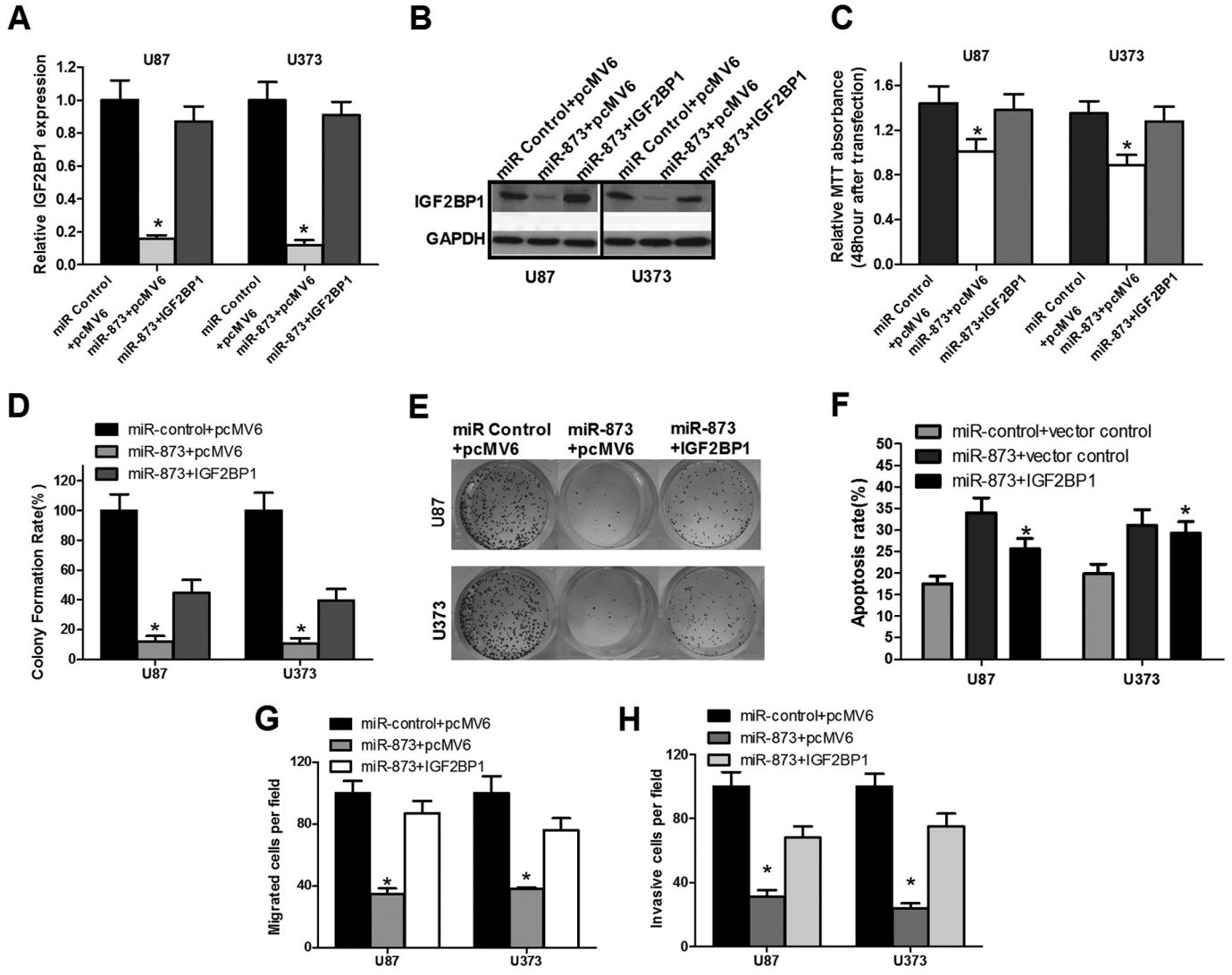

FIGURE 5. **The inhibition of cell growth and invasion caused by miR-873 was reversed by the overexpression of IGF2BP1 in GBM cells.** *A*, the relative expression levels of IGF2BP1 were detected in the GBM cells transfected with miR-873 or control mimics and in cells co-transfected with miR-873 and pcMV6.0/IGF2BP1 using quantitative RT-PCR. *B*, the relative protein levels of IGF2BP1 were determined using Western blot in the GBM cells transfected with miR-873 or control mimics and in cells co-transfected with miR-873 and pcMV6/IGF2BP1. *C* and *D*, the ability of GBM cell transfected with miR-873 or control mimics and co-transfected with miR-873 and pcMV6/IGF2BP1, measured by MTT or colony formation assays. *E*, the representative colony images were shown. *F*, Apoptosis assay was performed in each group of transfected GBM cells. *G* and *H*, the migration and invasion abilities of the GBM cells transfected with miR-873 or control mimics and cells co-transfected with miR-873 and pcMV6/IGF2BP1 are presented using Transwell assays. The experiments were performed in triplicate. *Error bars* indicate S.D. *, $p < 0.05$.

DISCUSSION

Malignant gliomas are the most aggressive and fatal tumors arising in the central nervous system, and GBM is the most cytologically malignant and active primary brain tumor (22, 23). The low survival rates of malignant gliomas are related to treatment difficulties, the lack of clinical, radiologic, and morphologic forewarning, and their infiltrating natures (24–27). miRNAs can either positively or negatively affect the development of GBM depending on their specific downstream target genes. Although miR-21, miR-221, and miR-10b have been identified as up-regulated and reported to function as oncogenic miRNAs in GBM tumors (28–30), several miRNAs, including miR-34a, miR-218, and miR-128, are down-regulated and act as tumor suppressors in GBM (12, 31, 32). The down-regulation of miR-873 in GBM has been demonstrated using cluster analysis (16). Accordingly, we used real-time RT-PCR assays to demonstrate that the expression of miR-873 was significantly down-regulated in GBM tumor tissues and cell lines (Fig. 1). The transfection of U87 and U373 cells with miR-873 mimics inhibited GBM cell proliferation but also increased their apoptosis rates (Fig. 2). Furthermore, the high cellular level of miR-873 negatively affected GBM cell migration and invasion (Fig. 3). Using bioinformatic tools, IGF2BP1 was identified as a potential target gene of miR-873 (Fig. 4). The decreased luciferase reporter signal in cells expressing the 3′-UTR of IGF2BP1 showed that miR-873 could suppress the target gene expression by directly binding to its 3′-UTR (Fig. 4*C*). The suppressive role of miR-873 in the expression of IGF2BP1 was supported by the down-regulation of IGF2BP1 expression caused by the transfection of GBM cells with miR-873 mimics (Fig. 4, *D* and *E*). Three potential binding sites flank the 3′-UTR of the IGF2BP mRNA transcript. Putative site 1 was predicted

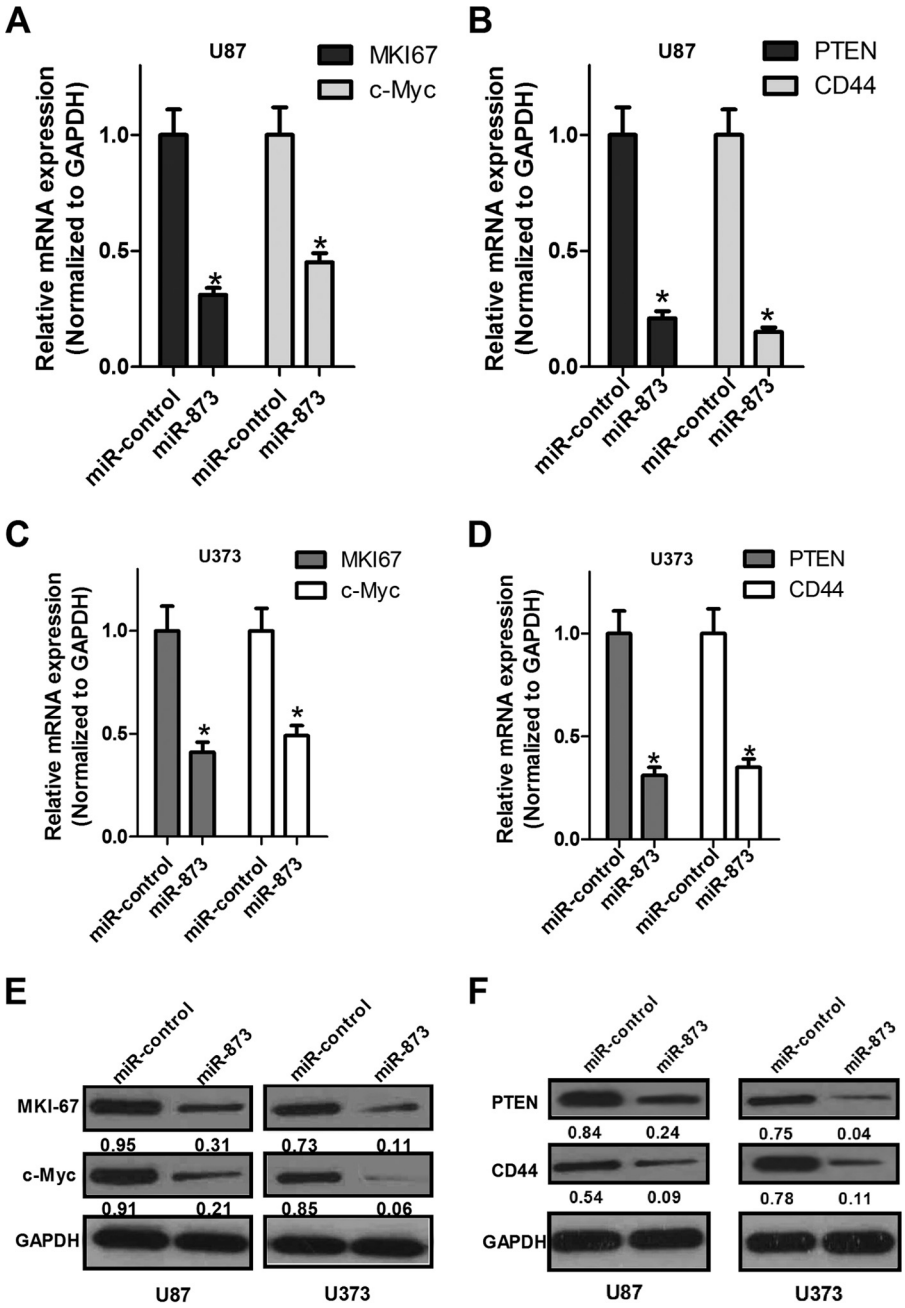

FIGURE 6. **The up-regulation of miR-873 suppresses the expression of MKI67, C-MYC, PTEN, and CD44 in GBM cells.** *A*, the levels of MKI67 and c-MYC mRNA in U87 cells after transfection with miR-873 mimics or control mimics were analyzed by real-time RT-PCR. *B*, the levels of PTEN and CD44 mRNA in U87 cells transfected with miR-873 mimics or control mimics were analyzed by real-time RT-PCR. *C*, the levels of MKI67 and c-MYC mRNA in U373 cells transfected with miR-873 mimics or control mimics were analyzed by real-time RT-PCR. *D*, the levels of PTEN and CD44 mRNA in U373 cells transfected with miR-873 mimics or control mimics were analyzed by real-time RT-PCR. *E*, the protein levels of MKI67 and c-MYC in U87 and U373 cells transfected with miR-873 mimics were determined relative to the corresponding cells transfected with control mimics by Western blotting. *F*, the protein levels of PTEN and CD44 in U87 and U373 cells transfected with miR-873 mimics were determined relative to the corresponding cells transfected with control mimics by Western blotting. GAPDH mRNA served as the control to determine the mRNA abundance relative to the controls, and GAPDH protein served as the control to determine the protein abundance. The statistical significance was determined with Student's *t* test: *, $p < 0.005$. *Error bars* indicate the S.D. of at least three independent analyses.

to be a major binding site of microRNA according to the mfe structure of the RNA duplex formed by miR-873 and its putative binding sequence using RNAhybrid. This binding was verified using Dual-Luciferase reporter assays. Fig. 4*C* shows that the mutation of putative site 1 resulted in the most obvious increase in the luciferase activity of the reporter vector containing the 3′-UTR mutant (IGF2BP1-3′-UTR mut) when compared with the activity of the vector containing the native 3′-UTR (IGF2BP1-3′-UTR WT) in GBM cells transfected with miR-873 mimics. Moreover, we discovered that the overexpression of IGF2BP1 partially mitigated the protective effects of miR-873 overexpression on the tumorigenic properties of glioma cell lines (Fig. 5, *A–H*). These results suggest that the regulation of IGF2BP1 levels by miR-873 is partly responsible for GBM progression in GBM tumors with reduced levels of miR-873.

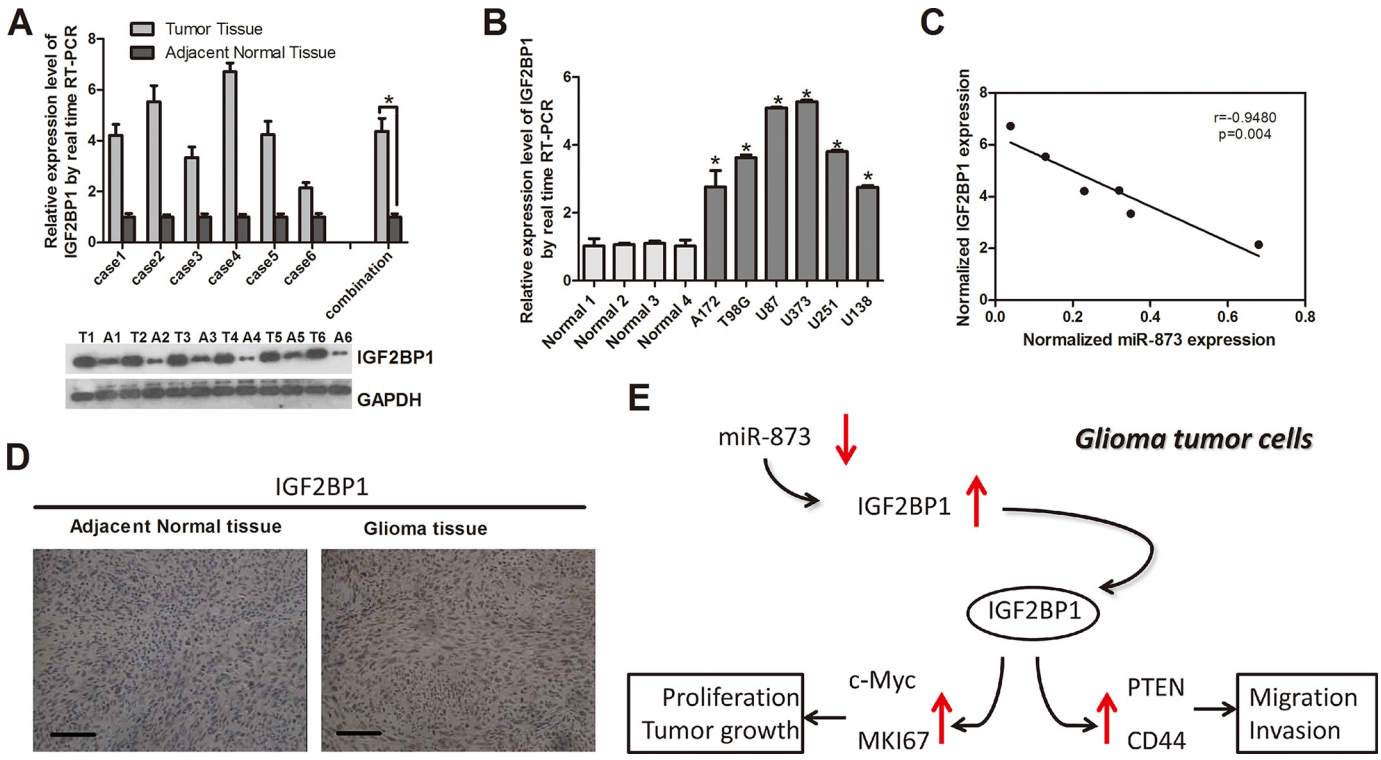

FIGURE 7. **The up-regulation of IGF2BP1 expression caused by the decreased level of miR-873 expression is involved in the progression of GBM.** *A*, analysis of IGF2BP1 in GBM tissues and adjacent normal tissues. *B*, analysis of IGF2BP1 in GBM cell lines and normal cells. *C*, the inverse relationship between the expression of IGF2BP1 and miR-873. *D*, GBM and normal ones tissues were stained with specific antibodies to IGF2BP1. Representative micrographs were framed and enlarged. *E*, the suggested molecular mechanism of the tumorigenesis and metastasis of GBM. *Error bars* indicate the S.E. of at least three independent analyses.

IGF2BP1 is expressed during embryogenesis, but this protein is also synthesized in a broad variety of malignancies (33). The expression of IGF2BP1 was associated with an overall poor prognosis in a wide range of cancers, suggesting that the protein may act as a potent oncogenic factor (34, 35). Accordingly, we observed that IGF2BP1 expression was up-regulated in tumor tissue (Fig. 7, *A*, *B*, and *D*). IGF2BP1 stabilized mRNA by binding to the target sequence in the mRNA transcript. IGF2BP1 prevented c-MYC mRNA degradation by binding to the coding region determinant located at the open reading frame and prolonged the half-life of CD44 mRNA by associating with the 3′-untranslated region of the transcript (20). Two novel target transcripts of IGF2BP1 protein, PTEN and MARK4, were discovered using a comparative microarray and verified using quantitative RT-PCR (17). Recently, researchers reported that IGF2BP1 stabilized c-MYC and MKI67 mRNAs and enhanced the expression of c-MYC and Ki-67 protein, which are both potent regulators of cell proliferation and apoptosis (17). In our study, the expression of IGF2BP1 target transcripts, including MKI67, c-MYC, PTEN, and CD44 mRNA, was down-regulated after the transfection of GBM cells with miR-873 mimics (Fig. 6, *A*–*F*). Therefore, the inhibition of IGF2BP1 expression by miR-873 in GBM cells down-regulated the expression of the downstream target transcripts of IGF2BP1. The overexpression of c-MYC, a proto-oncogene, has been reported in human GBM (36). IGF2BP1 has been suggested as a potent oncogenic factor that is involved in tumor cell proliferation by stabilizing c-MYC mRNA in carcinoma cells (21). IGF2BP1 promoted invadopodia formation by preventing CD44 mRNA degradation (20). The deletion of PTEN in early neural precursors resulted in marked neuronal migration defects (37, 38). IGF2BP1 enhanced the directionality of cell migration in a functional PTEN-dependent manner. These findings supported the hypothesis that the decreased level of miR-873 promoted the carcinogenesis and metastasis of GBM by up-regulating the expression of IGF2BP1 protein and its target RNA transcripts, including IGF2BP1, MKI67, c-MYC, PTEN, and CD44 mRNA (Fig. 7*E*).

In conclusion, the major findings of this study can be summarized as follows. (*a*) miR-873 was down-regulated in GBM tissues and cell lines. (*b*) We have shown for the first time that miR-873 directly targets IGF2BP1 and down-regulates the expression of IGF2BP1 in GBM cells via the first binding site in its 3′-UTR. (*c*) The ectopic expression of miR-873 markedly inhibited the proliferation and invasion of GBM cell lines, and this phenotype was mediated by the miR-873/IGF2BP1 signaling pathway. (*d*) The ectopic expression of miR-873 could regulate MKI67, c-MYC, PTEN, and CD44 mRNA via IGF2BP1. These results provide strong evidence that miR-873 acts as a tumor suppressor in GBM development by regulating IGF2BP1 and may implicate miR-873 as a potential target for GBM therapy.

REFERENCES

1. Gladson, C. L., Prayson, R. A., and Liu, W. M. (2010) The pathobiology of glioma tumors. *Annu. Rev. Pathol.* **5,** 33–50
2. Kohler, B. A., Ward, E., McCarthy, B. J., Schymura, M. J., Ries, L. A., Eheman, C., Jemal, A., Anderson, R. N., Ajani, U. A., and Edwards, B. K. (2011) Annual report to the nation on the status of cancer, 1975–2007,

featuring tumors of the brain and other nervous system. *J. Natl. Cancer Inst.* **103,** 714–736
3. Furnari, F. B., Fenton, T., Bachoo, R. M., Mukasa, A., Stommel, J. M., Stegh, A., Hahn, W. C., Ligon, K. L., Louis, D. N., Brennan, C., Chin, L., DePinho, R. A., and Cavenee, W. K. (2007) Malignant astrocytic glioma: genetics, biology, and paths to treatment. *Genes Dev.* **21,** 2683–2710
4. Singh, S. K., Hawkins, C., Clarke, I. D., Squire, J. A., Bayani, J., Hide, T., Henkelman, R. M., Cusimano, M. D., and Dirks, P. B. (2004) Identification of human brain tumour initiating cells. *Nature* **432,** 396–401
5. Ohgaki, H., and Kleihues, P. (2005) Epidemiology and etiology of gliomas. *Acta Neuropathol.* **109,** 93–108
6. Bartel, D. P. (2004) MicroRNAs: genomics, biogenesis, mechanism, and function. *Cell* **116,** 281–297
7. Ambros, V. (2004) The functions of animal microRNAs. *Nature* **431,** 350–355
8. Ciafrè, S. A., Galardi, S., Mangiola, A., Ferracin, M., Liu, C. G., Sabatino, G., Negrini, M., Maira, G., Croce, C. M., and Farace, M. G. (2005) Extensive modulation of a set of microRNAs in primary glioblastoma. *Biochem. Biophys. Res. Commun.* **334,** 1351–1358
9. Chan, J. A., Krichevsky, A. M., and Kosik, K. S. (2005) MicroRNA-21 is an antiapoptotic factor in human glioblastoma cells. *Cancer Res.* **65,** 6029–6033
10. Papagiannakopoulos, T., Shapiro, A., and Kosik, K. S. (2008) MicroRNA-21 targets a network of key tumor-suppressive pathways in glioblastoma cells. *Cancer Res.* **68,** 8164–8172
11. Gabriely, G., Yi, M., Narayan, R. S., Niers, J. M., Wurdinger, T., Imitola, J., Ligon, K. L., Kesari, S., Esau, C., Stephens, R. M., Tannous, B. A., and Krichevsky, A. M. (2011) Human glioma growth is controlled by microRNA-10b. *Cancer Res.* **71,** 3563–3572
12. Tu, Y., Gao, X., Li, G., Fu, H., Cui, D., Liu, H., Jin, W., and Zhang, Y. (2013) MicroRNA-218 inhibits glioma invasion, migration, proliferation, and cancer stem-like cell self-renewal by targeting the polycomb group gene *Bmi1*. *Cancer Res.* **73,** 6046–6055
13. Hui, W., Yuntao, L., Lun, L., WenSheng, L., ChaoFeng, L., HaiYong, H., and Yueyang, B. (2013) MicroRNA-195 inhibits the proliferation of human glioma cells by directly targeting cyclin D1 and cyclin E1. *PLoS One* **8,** e54932
14. Sun, G., Cao, Y., Shi, L., Sun, L., Wang, Y., Chen, C., Wan, Z., Fu, L., and You, Y. (2013) Overexpressed miRNA-137 inhibits human glioma cells growth by targeting Rac1. *Cancer Biother. Radiopharm.* **28,** 327–334
15. Yang, T. Q., Lu, X. J., Wu, T. F., Ding, D. D., Zhao, Z. H., Chen, G. L., Xie, X. S., Li, B., Wei, Y. X., Guo, L. C., Zhang, Y., Huang, Y. L., Zhou, Y. X., and Du, Z. W. (2014) MicroRNA-16 inhibits glioma cell growth and invasion through suppression of BCL2 and the nuclear factor-κB1/MMP9 signaling pathway. *Cancer Sci.* **105,** 265–271
16. Skalsky, R. L., and Cullen, B. R. (2011) Reduced expression of brain-enriched microRNAs in glioblastomas permits targeted regulation of a cell death gene. *PLoS One* **6,** e24248
17. Gutschner, T., Hämmerle, M., Pazaitis, N., Bley, N., Fiskin, E., Uckelmann, H., Heim, A., Groß, M., Hofmann, N., Geffers, R., Skawran, B., Longerich, T., Breuhahn, K., Schirmacher, P., Mühleck, B., Hüttelmaier, S., and Diederichs, S. (2014) Insulin-like growth factor 2 mRNA-binding protein 1 (IGF2BP1) is an important protumorigenic factor in hepatocellular carcinoma. *Hepatology* **59,** 1900–1911
18. Sotgia, F., Razani, B., Bonuccelli, G., Schubert, W., Battista, M., Lee, H., Capozza, F., Schubert, A. L., Minetti, C., Buckley, J. T., and Lisanti, M. P. (2002) Intracellular retention of glycosylphosphatidyl inositol-linked proteins in caveolin-deficient cells. *Mol. Cell. Biol.* **22,** 3905–3926
19. Sparanese, D., and Lee, C. H. (2007) CRD-BP shields c-*myc* and *MDR*-1 RNA from endonucleolytic attack by a mammalian endoribonuclease. *Nucleic Acids Res.* **35,** 1209–1221
20. Vikesaa, J., Hansen, T. V., Jønson, L., Borup, R., Wewer, U. M., Christiansen, J., and Nielsen, F. C. (2006) RNA-binding IMPs promote cell adhesion and invadopodia formation. *EMBO J.* **25,** 1456–1468
21. Stöhr, N., Köhn, M., Lederer, M., Glass, M., Reinke, C., Singer, R. H., and Hüttelmaier, S. (2012) IGF2BP1 promotes cell migration by regulating MK5 and PTEN signaling. *Genes Dev.* **26,** 176–189
22. Louis, D. N., Ohgaki, H., Wiestler, O. D., Cavenee, W. K., Burger, P. C., Jouvet, A., Scheithauer, B. W., and Kleihues, P. (2007) The 2007 WHO classification of tumours of the central nervous system. *Acta Neuropathol.* **114,** 97–109
23. Ohgaki, H., and Kleihues, P. (2005) Population-based studies on incidence, survival rates, and genetic alterations in astrocytic and oligodendroglial gliomas. *J. Neuropathol. Exp. Neurol.* **64,** 479–489
24. Kanu, O. O., Hughes, B., Di, C., Lin, N., Fu, J., Bigner, D. D., Yan, H., and Adamson, C. (2009) Glioblastoma multiforme oncogenomics and signaling pathways. *Clin. Med. Oncol.* **3,** 39–52
25. Ostrom, Q. T., and Barnholtz-Sloan, J. S. (2011) Current state of our knowledge on brain tumor epidemiology. *Curr. Neurol. Neurosci. Rep.* **11,** 329–335
26. Stupp, R., Hegi, M. E., Mason, W. P., van den Bent, M. J., Taphoorn, M. J., Janzer, R. C., Ludwin, S. K., Allgeier, A., Fisher, B., Belanger, K., Hau, P., Brandes, A. A., Gijtenbeek, J., Marosi, C., Vecht, C. J., Mokhtari, K., Wesseling, P., Villa, S., Eisenhauer, E., Gorlia, T., Weller, M., Lacombe, D., Cairncross, J. G., Mirimanoff, R. O., European Organisation for Research and Treatment of Cancer Brain Tumour and Radiation Oncology Groups, and National Cancer Institute of Canada Clinical Trials Group (2009) Effects of radiotherapy with concomitant and adjuvant temozolomide versus radiotherapy alone on survival in glioblastoma in a randomised phase III study: 5-year analysis of the EORTC-NCIC trial. *Lancet Oncol.* **10,** 459–466
27. Kang, M. K., and Kang, S. K. (2007) Tumorigenesis of chemotherapeutic drug-resistant cancer stem-like cells in brain glioma. *Stem Cells Dev.* **16,** 837–847
28. Conti, A., Aguennouz, M., La Torre, D., Tomasello, C., Cardali, S., Angileri, F. F., Maio, F., Cama, A., Germanò, A., Vita, G., and Tomasello, F. (2009) miR-21 and 221 upregulation and miR-181b downregulation in human grade II-IV astrocytic tumors. *J. Neurooncol.* **93,** 325–332
29. Guessous, F., Alvarado-Velez, M., Marcinkiewicz, L., Zhang, Y., Kim, J., Heister, S., Kefas, B., Godlewski, J., Schiff, D., Purow, B., and Abounader, R. (2013) Oncogenic effects of miR-10b in glioblastoma stem cells. *J. Neurooncol.* **112,** 153–163
30. Zhou, X., Ren, Y., Moore, L., Mei, M., You, Y., Xu, P., Wang, B., Wang, G., Jia, Z., Pu, P., Zhang, W., and Kang, C. (2010) Downregulation of miR-21 inhibits EGFR pathway and suppresses the growth of human glioblastoma cells independent of PTEN status. *Lab. Invest.* **90,** 144–155
31. Godlewski, J., Nowicki, M. O., Bronisz, A., Williams, S., Otsuki, A., Nuovo, G., Raychaudhury, A., Newton, H. B., Chiocca, E. A., and Lawler, S. (2008) Targeting of the Bmi-1 oncogene/stem cell renewal factor by microRNA-128 inhibits glioma proliferation and self-renewal. *Cancer Res.* **68,** 9125–9130
32. Guessous, F., Zhang, Y., Kofman, A., Catania, A., Li, Y., Schiff, D., Purow, B., and Abounader, R. (2010) microRNA-34a is tumor suppressive in brain tumors and glioma stem cells. *Cell Cycle* **9,** 1031–1036
33. Yaniv, K., and Yisraeli, J. K. (2002) The involvement of a conserved family of RNA binding proteins in embryonic development and carcinogenesis. *Gene* **287,** 49–54
34. Vainer, G., Vainer-Mosse, E., Pikarsky, A., Shenoy, S. M., Oberman, F., Yeffet, A., Singer, R. H., Pikarsky, E., and Yisraeli, J. K. (2008) A role for VICKZ proteins in the progression of colorectal carcinomas: regulating lamellipodia formation. *J. Pathol.* **215,** 445–456
35. Köbel, M., Weidensdorfer, D., Reinke, C., Lederer, M., Schmitt, W. D., Zeng, K., Thomssen, C., Hauptmann, S., and Hüttelmaier, S. (2007) Expression of the RNA-binding protein IMP1 correlates with poor prognosis in ovarian carcinoma. *Oncogene* **26,** 7584–7589
36. Trent, J., Meltzer, P., Rosenblum, M., Harsh, G., Kinzler, K., Mashal, R., Feinberg, A., and Vogelstein, B. (1986) Evidence for rearrangement, amplification, and expression of c-*myc* in a human glioblastoma. *Proc. Natl. Acad. Sci. U.S.A.* **83,** 470–473
37. Fraser, M. M., Zhu, X., Kwon, C. H., Uhlmann, E. J., Gutmann, D. H., and Baker, S. J. (2004) Pten loss causes hypertrophy and increased proliferation of astrocytes *in vivo*. *Cancer Res.* **64,** 7773–7779
38. Yue, Q., Groszer, M., Gil, J. S., Berk, A. J., Messing, A., Wu, H., and Liu, X. (2005) PTEN deletion in Bergmann glia leads to premature differentiation and affects laminar organization. *Development* **132,** 3281–3291